Asociación Argentina
de Mecánica Computacional

Mecánica Computacional Vol XXIX, págs. 4967-4975 (artículo completo)
Eduardo Dvorkin, Marcela Goldschmit, Mario Storti (Eds.)
Buenos Aires, Argentina, 15-18 Noviembre 2010

# A COMPARISON OF BUCKLING PERFORMANCE OF RIVET AND FRICTION STIR WELDING STIFFENED PANELS

**Eliseu Lucena Neto, Francisco A. C. Monteiro and Hugo H. Ruela**

*Instituto Tecnológico de Aeronáutica, Praça Marechal Eduardo Gomes 50, 12228-900, São José dos Campos, Brasil, eliseu@ita.br, http://www.civil.ita.br*

**Keywords:** Friction stir welding, Buckling analysis, Stiffened panels.

**Abstract.** The introduction of friction stir welding (FSW) as an alternative joining process for traditional rivet fastening for primary aircraft structures has the potential to lower manufacturing costs and structural weight. Methods for strength analysis and design are currently under development. In this context, the present work aims to highlight the main differences between local buckling strength behavior of FSW and rivet stiffened panels. Several stiffener panels, with a variable number of stiffeners and joining type, subject to uniform compression are numerically tested utilizing finite element models. The obtained results are compared to simplified analytical results currently employed in design. A first insight on the critical buckling performance between riveted and welded designs is then allowed.

## 1 INTRODUCTION

The reduction in design, manufacture and maintenance costs is a fundamental aerospace engineering task. Towards this objective new manufacturing processes have been developed in last decade, e.g., friction stir welding, electron beam welding, laser beam welding. Many investigations has been carried out in order to implementing these new welding processes on aircraft projects to replace the old-fashioned riveted connections. However, significant residual stress, plastic deformation and material property changes occur simultaneously, despite the advanced welding machinery.

Introduction of inherent material imperfections by welding process leads naturally to a more complicated analysis procedure. In a structural analysis viewpoint, the major restriction for implementation of advanced welding processes to full manufacture of aircraft structures is the lack of basic knowledge about welding effects on stiffened panel strength performance. To date it has been a common design practice to apply empirically determined knock-down factors to account for all welding effects. In order to establish design rules and analysis tools, the industry and academic researchers have studied and identified the dominant welding effects and their influence on strength performance by means of a series of experimental tests programs. Appropriated methods for strength analysis have been proposed to aeronautical welding panels, as well as manufacturing process parameter optimisation for reliable welds (Gibson and Sterling, 1998; Dracup and Arbegast, 1999; Hoffman et al., 2002; Murphy et al., 2006) .

The friction stir welding (FSW) is a solid-state joining process that present superior mechanical properties, lower residual stresses and distortions, being a potential lower cost replacement for the riveted construction of aircraft primary structures, like fuselage skin-stiffener connection. The FSW fuselage skin-stiffener connection is obtained by inserting a specially designed rotating pin over the stiffener flange to be welded, and then moving the pin along its length. The designer is commonly restricted to specify only stiffeners with Z or hat sections because of the tooling limitation. Heat is generated by the rotating tool both by frictional forces and due to deformation of the stringer and skin material. Moreover, the combination of the tool spin and feed rate determines the metal flow around the tool contact surface (Guerra et al., 2003; Liu et al., 2003) . Figure 1 presents a schematic view of weld zones. Examination of the resulting material microstructure at weld location, three distinct regions which vary gradually could be identified (Murphy et al., 2007; Yoon et al., 2009) :

- parent material zone (PMZ) where no thermal deformation has occurred and the heat flux has not affected the mechanical properties;
- heat affected zone (HAZ) where no thermal deformation has occurred, but material properties have been modified due to heat flux (experimental data have measured a degradation range of $65\%$ - $95\%$ of the parent material properties). The HAZ extends symmetrically from the centre line of the connection flange approximatelly $6$ to $12$ times the thickness of the welded through flange;
- thermo-mechanically affected zone (TMAZ) in which occur both thermal deformation and material properties degeneration. The TMAZ actually defines the weld joint width and varies from $2$ to $6$ times the thickness of the welded through flange. The bulk zone, namely, the weld nugget, defines itself a TMAZ subzone due to the recrystallized microstructure significantly different from vicinity.

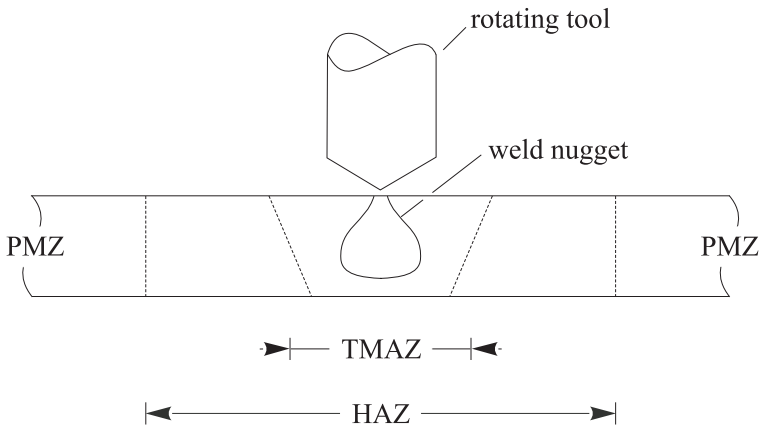


Figure 1: Schematic view of weld zones.

In a traditional riveted connection, the structural assembly is made by means of a mechanical joint, for instance, splices and fittings. The FSW process provides a way to achieve this without adding additional mechanical joints and significant weight to the structure. Furthermore, friction stir weldings may also have better fatigue performance than mechanical joints and have been found to retard fatigue crack growth, due to the presence of beneficial residual stresses in the weld zone (Fratini et al., 2009; Lemmen et al., 2010) .

To evaluate the potential of friction stir welding as a replacement for traditional rivet fastening for launch vehicle dry bay construction, Lockheed-Martin Space Systems as part of NASA investigation have designed and fabricated a large-scale friction stir welded 2090-T83 aluminum-lithium (Al-Li) alloy skin-stiffener panel (Hoffman et al., 2002) . The friction stir welded panel and a conventional riveted panel were tested to failure in compression. The research has considered specimens with stiffeners of a hat section profile. Both the riveted and FSW panel experienced initial skin buckling at loads well below predicted values. The authors have pointed out several factors to explain this behavior including distortion, geometric imperfections, and reduced weldment properties. It was achieved that distortion played a significant role in the FSW panel performance. Due to the welding imperfections the FSW panel failure load was 5% less than the predicted analysis value, whereas the riveted panel ultimate load strenght has attained higher value than the predicted one (the welded panel had a 20% lower failure load than the equivalent riveted panel).

Utilising experimentally validated finite element models, Murphy et al. (2007) have also demonstrated that local skin buckling of stiffener FSW panels was mainly influenced by the magnitude of welding induced residual stresses and associated geometric distortions. In addition, they have concluded that the post-buckling performance was less sensitive to the applied process effects and process effect magnitudes than initial buckling. The local buckling behavior of a FSW integrally stiffened panel structure was investigated by Yoon et al. (2009) . The authors have employed the Ramberg-Osgood constitutive model to access the material inelastic range, and all parent material degradation into HAZ was accounted for by introducing only a single reduction factor on the yield reference stress value.

The presented work aims to highlight the main differences between local buckling behavior of FSW and riveted stiffened panels. Several stiffener flat panels with a variable number of stiffeners and joining type, subject to uniform compression, are numerically tested by a finite element model (FEM). The panel geometry is representative of panel structure found on the lower fuselage belly of a commercial aircraft. A first insight on the critical buckling perfor-

mance between riveted and welded designs is then allowed.

## 2 STIFFENED PANEL MODEL

When examinning the buckling performance of a welded stiffened panel like the one depicted in Fig. 2, geometric and material imperfections should be regarded. These imperfections can be subdivided into the following categories:

1. skin transverse deflection (skin out-of-plane deflection between longitudinal stiffeners)
2. stiffener lateral deflection (web out-of-plane deflection)
3. skin welding resulting residual stress
4. stiffener welding resulting residual stress
5. material HAZ extension and degradation level.

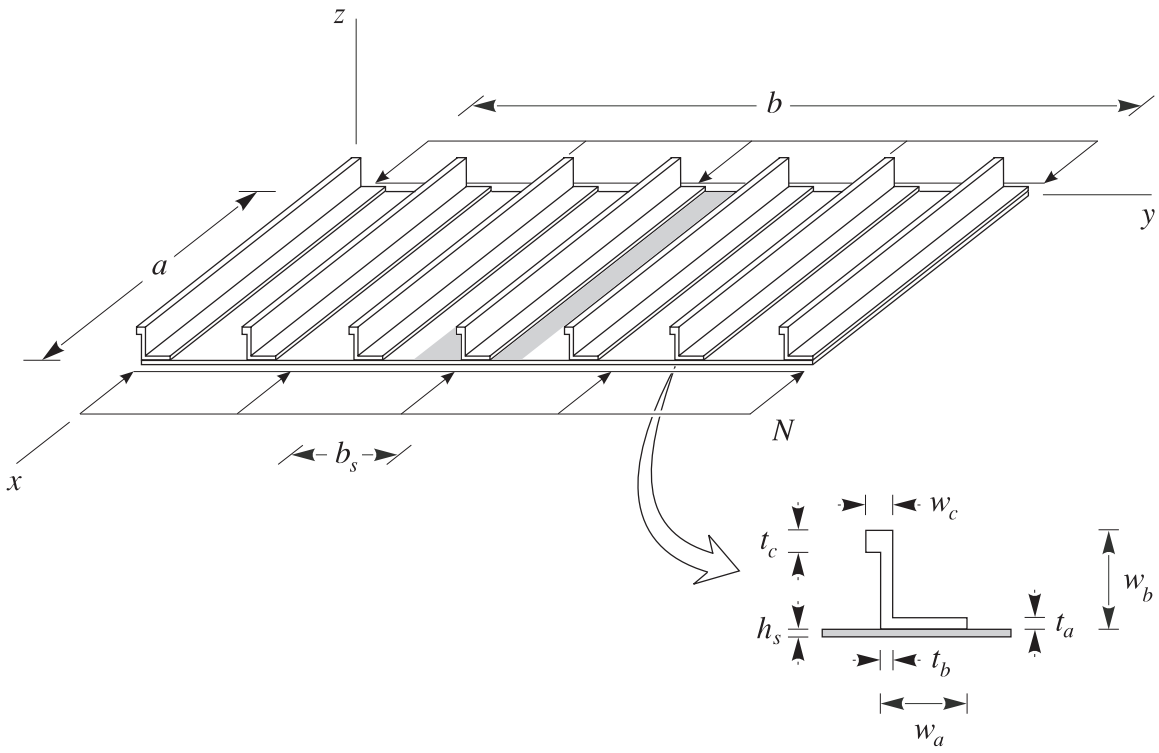


Figure 2: Welded stiffened panel subjected to uniform compression loading.

For practical purposes, the buckling behavior of riveted panels is controlled by the geometric imperfections 1-3 only. It is a complicated task to consider all imperfections into a design analysis model. Indeed, to determine the actual buckling strength of an imperfect structure a fully nonlinear buckling analysis needs to be performed, and the algorithm solution should be able to identify the structure critical points (Crisfield, 1991; Bažant and Cedolin, 2003) .

Assuming that loss of equilibrium stability occurs at a bifurcation point in the vicinity of the flat configuration, evaluation of the panel critical load could be done by a linear buckling analysis of the perfect structure in order to gain a first insight on the critical performance between FSW and riveted stiffened panels. All material welding resulting imperfections could be

taken into account, in a simplified manner, by an appropriated degradation of the HAZ material elastic modulus.

For eigenvalue buckling analysis, a series of one-bay panels with different number of equally spaced longitudinal Z-stiffeners was modeled and analyzed using the finite element commercial code NASTRAN (MSC, 2008) . To prevent edge buckling, additional stiffeners were attached to the longitudinal edges of the panel which resulted in realistic uniform local plate buckling between the stiffeners. The skin is subjected to a uniaxial compressive load $N$ (Fig. 2), and its edges are supposed to be simply supported (Fig. 3). The panel skin and longitudinal stiffeners are made of aluminum alloys commonly used in aeronautical applications, with mechanical properties described in Table 1 (DOD, 1998) . The geometrical data of the panels with three, four and five stiffeners (including the edge ones) are listed in Table 2. All the analysed panels have the same lenght and two different assigned width to evaluate the influence of panel aspect ratio. Table 3 presents the cross-sectional dimensions of the Z-stiffeners.

| Material | Type | $E$ (MPa) | $\nu$ |
|---|---|---|---|
| Skin | AL 2024-T3 | 72400 | 0.33 |
| Stiffener | AL 7050-T3511 | 71020 | 0.33 |

Table 1: Material properties.

| Painel ID | $a$ (mm) | $b$ (mm) | $h_s$ (mm) | N. stiffeners |
|---|---|---|---|---|
| 1 | 700 | 840 | 1 | 3 |
| 2 | 700 | 560 | 1 | 3 |
| 3 | 700 | 840 | 1 | 4 |
| 4 | 700 | 560 | 1 | 4 |
| 5 | 700 | 840 | 1 | 5 |
| 6 | 700 | 560 | 1 | 5 |

Table 2: Panels geometrical data.

| Width (mm) | | Thickness (mm) | |
|---|---|---|---|
| $w_a$ | 19.05 | $t_a$ | 1.27 |
| $w_b$ | 19.05 | $t_b$ | 1.27 |
| $w_c$ | 5.5 | $t_c$ | 3.00 |

Table 3: Stiffener cross-sectional dimensions.

Except the stiffener upper flange, that is modeled using the simple beam element CBAR, the rest of panel structure are meshed with quadrilateral plate elements CQUAD4. The stiffened panel is discretized into sufficient number of elements to allow for free development of the buckling modes. A quadrialteral $4 \times 88$ element mesh is employed along the stiffener web/connected flange and at the underneath skin, whereas a $48 \times 88$ element mesh is employed between longitudinal stiffeners. No attempt was made to optimise the mesh. A five-stiffener model is shown in Fig. 4.

An appropriated representation for the buckling modes of an aircraft fuselage panel is obtained if a realistc representation of the skin and stiffener joint area is carried out. With this in mind, a simple procedure to representate the FSW joint is outlined in what follows. First, the

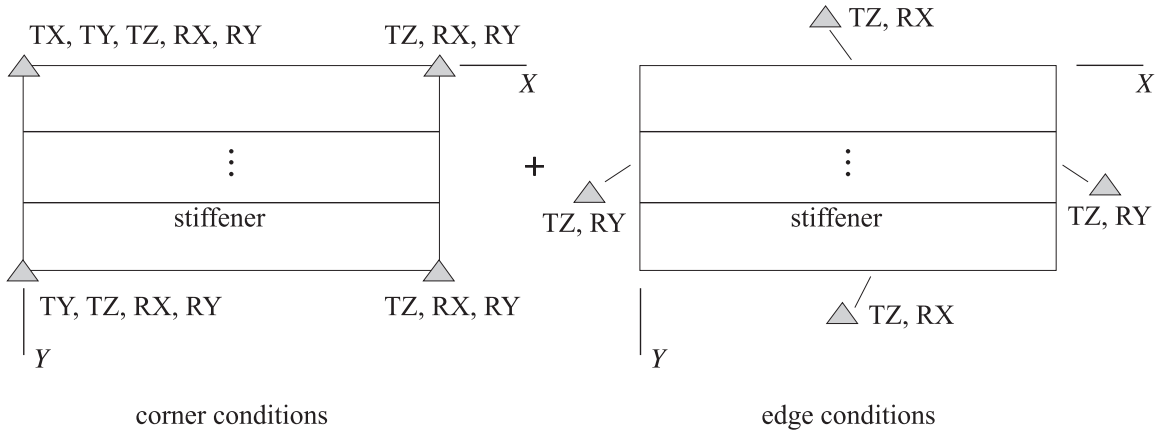


Figure 3: Panel boundary conditions.

TMAZ width is considered to be null and the weld is assumed to be a line that join continuously the flange center node to its projection node on skin. Second, to simulate the monolithic behavior of a FSW connection, the nodes in the skin and stiffener weld joint area are connected with RBE2 rigid elements. Only the translational displacements degrees-of-freedom of the connected nodes are rigidly attached. Finally, the contact conditions between the unwelded skin and stiffener flange are modelled using a uniaxial linear gap scheme as shown in Fig. 5a.

In relation to the riveted conections, the concept of joint stiffness plays a fundamental role. The joint stiffness is a measure of the influence of fasteners (rivets, bolts, etc.) on the rigidity of joints between the sheets of material from which most aircraft are constructed. It influences the fatigue life of an aircraft joint, and is often used as a parameter when modelling and analysing aircraft with regards to fatigue and life-span. The transverse joint stiffness $K_t$ is calculated with the following empirical formula proposed by Swift (1979)

$$K_t = \left[ \frac{5}{E_r d_r} + \frac{4}{5} \left( \frac{1}{h_s E_s} + \frac{1}{t_a E} \right) \right]^{-1} \tag{1}$$

where $d_r$ is the rivet diameter and $E_r$, $E_s$, $E$ are the rivet, skin, stiffener Young´s modulus. The axial joint stiffness $K_a$ is calculated based on the rivet extensional rigidity

$$K_a = \frac{\pi E_r d_r^2}{2\,(h_s + t_a)}. \tag{2}$$

Transverse and axial joint stiffness are introduced into skin-stiffener connection finite element modelling by means of CELAS2 scalar spring elements as shown in Fig. 5b. The spring elements connect the flange center node to its projection node on skin. To model the joint transverse stiffness, two CELAS2 elements are placed at rivet locations within the appropriated spring constant defined by Eq. (1). Furthermore, one places a single CELAS2 element in order to access the joint axial stiffness, which spring constant is now given by Eq. (2). Finally, the contact conditions between the unriveted skin and stiffener flange are modelled using a series of uniaxial linear gaps.

The panel rivet type MS20470AD-5 is chosen due to its commonly use in aeronautical applications ($d_r = 3.97$ mm, $E_r = 71020$ MPa). In order to compare the local buckling performance of rivet and FSW panels, we have picked out the smallest riveting design pitch, i.e., $4 \times d_r = 15.9$ mm.

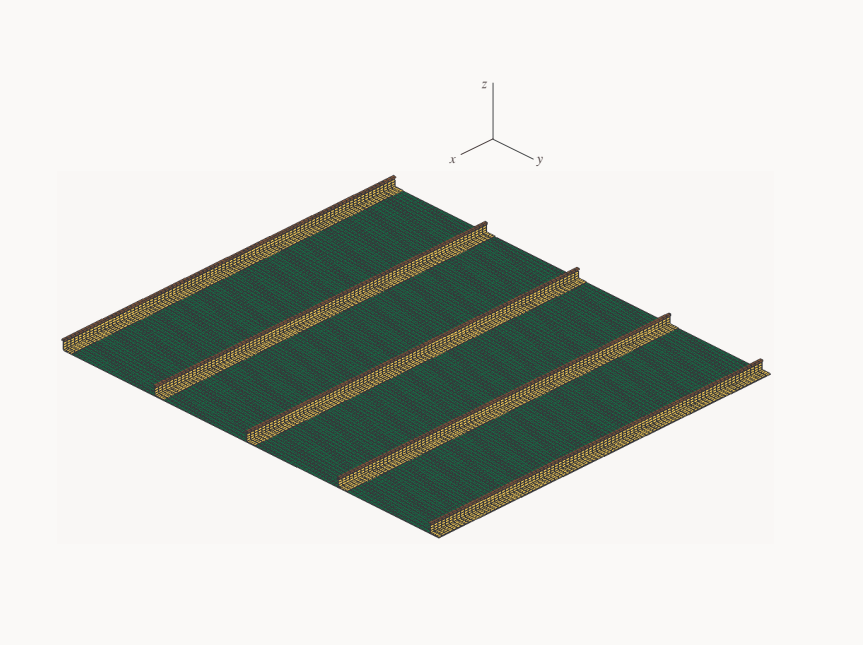


Figure 4: Finite element model for Z-shaped stiffened panels.

## 3 BUCKLING ANALYSIS

First, a buckling eigenvalue analysis are performed to compare the primary differences between FSW and riveted imperfection-free stiffened panels. Panels are loaded imposing a compressive uniformly distributed loading over plate width. Table 4 compares skin buckling loading for FSW and riveted skin-stiffener panels. The finite element results are compared with those obtained from an analytical buckling calculation that is based on a Rayleigh-Ritz type solution, which has been adapted from Bisagni and Vescovini (2009) .

When dealing with imperfection-free stiffened panels, it can be observed that: (i) the differences between linear buckling strength of FSW and rivet stiffened panels are negligible; (ii) the analyzed panels have experienced buckling loads well predicted by the analytical calculation, which have demonstrated a conservative accuracy.

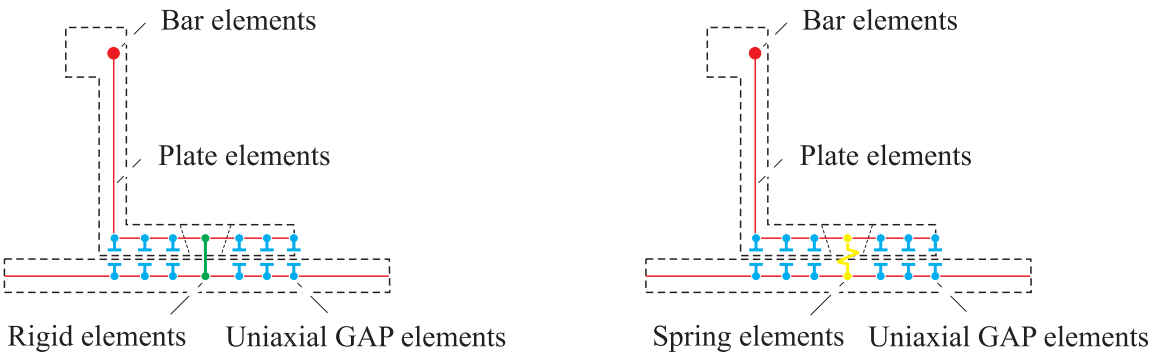


(a) FSW conection (b) Riveted conection

Figure 5: FE model joint idealization.

| | Buckling load (N/mm$^2$) | | | (FEM − Anal.)/Anal. × 100 | |
|---|---|---|---|---|---|
| Panel ID | FSW | Riveted | Analytical | FSW $vs$ Anal. | Riveted $vs$ Anal. |
| 1 | 2.0887 | 2.0920 | 2.0449 | 2.14 | 2.30 |
| 2 | 5.2779 | 5.2631 | 5.0354 | 4.82 | 4.52 |
| 3 | 5.0043 | 4.9908 | 4.9197 | 1.72 | 1.45 |
| 4 | 12.654 | 12.430 | 12.259 | 3.22 | 1.39 |
| 5 | 9.3636 | 9.2554 | 9.1889 | 1.90 | 0.72 |
| 6 | 23.723 | 22.838 | 22.679 | 4.60 | 0.70 |

Table 4: Comparison between results from finite element eigenvalue analysis for the FSW and riveted skin-stiffener imperfection-free panels.

In order to gain a first insight on the actual buckling performance of FSW panels, all material welding resulting imperfection is taken into account by a single degradation of the HAZ material elastic modulus. Assuming that the width of heat affected zone, $w_{HAZ}$, lies on the upper range of 12 times the thickness of the welded flange leads to $w_{HAZ} = 12t_a = 0.8w_a$. A conservative and simple approach is thus consider that the HAZ practically extends along the entire welded flange, $w_{HAZ} = w_a$.

Table 5 compares the buckling loads for FSW stiffened panels where the welding resulting material elastic modulus are assumed, respectively, $70\%$ and $80\%$ of the flange parent material property (FSW0.7 and FSW0.8) based on aluminum alloys weld efficiencies reported by Liu et al. (2003); Fioravanti (2008); Yoon et al. (2009) . The base metal skin material properties are considered unaffected by heat, and no initial geometric imperfections are introduced. Comparing the finite element results with those obtained from imperfection-free panels, it is observed that the differences between them are also negligible.

| | Buckling load (N/mm$^2$) | | |
|---|---|---|---|
| Panel ID | FSW0.7 | FSW0.8 | FSW |
| 1 | 2.0693 | 2.0759 | 2.0887 |
| 2 | 5.2042 | 5.2297 | 5.2779 |
| 3 | 4.9398 | 4.9619 | 5.0043 |
| 4 | 12.479 | 12.541 | 12.654 |
| 5 | 9.2301 | 9.2765 | 9.3636 |
| 6 | 23.415 | 23.504 | 23.723 |

Table 5: Comparison between results from finite element eigenvalue analysis for FSW stiffened panels considering material HAZ extension and degradation level.

## 4 CONCLUSIONS

The presented work aims to highlight the main differences between local buckling behavior of FSW and riveted stiffened panels. Several stiffened flat panels with a variable number of stiffeners and joint types, subject to uniform compression, are numerically tested utilizing a simplified finite element model. With respect to local buckling it was concluded that differences between friction stir welding and riveting manufacture processes are negligible when considering imperfection-free panels, and material heat affected zone extension/degradation level. The

inclusion of other imperfection types, for instance, the skin welding resulting residual stress, are necessary to access the actual FSW local buckling strength.

## REFERENCES


Bažant Z.P. and Cedolin L. *Stability of structures: elastic, inelastic, fracture, and damage theories*. Dover, Mineola, 2003.

Bisagni C. and Vescovini R. Analytical formulation for local buckling and post-buckling analysis of stiffened laminated panels. *Thin-Walled Structures*, 47:318–334, 2009.

Crisfield M.A. *Non-linear finite element analysis of solids and structures*, volume I. New York, NY: Wiley, 1991.

DOD U.S. *Metallic materials and elements for aerospace vehicle structures, MIL-HDBK-5H*. Defense Area Printing Service - DAPS, 1998.

Dracup B.J. and Arbegast W.J. Friction stir welding as a rivet replacement technology. In: Proceedings of the 1999 SAE Aerospace Automated Fastening Conference and Exposition, 1999.

Fioravanti A.S. *Soldagem por FSW de ligas de alumínio ALCLAD AA2024-T3 e AA7075-T6*. Master's Thesis, Universidade Federal do Rio Grande do Sul. Escola de Engenharia. Programa de Pós-Graduação em Engenharia Mecânica, 2008.

Fratini L., Pasta S., and Reynolds A.P. Fatigue crack growth in 2024-T351 friction stir welded joints: Longitudinal residual stress and microstructural effects. *International Journal of Fatigue*, 31:495–500, 2009.

Gibson A. and Sterling S. A design and test programme involving welded sheet-stringer compression panels. In: Proceedings of the International Council of the Aeronautical Sciences ICAS 1998, 1998.

Guerra M., Schmidt C., McClure J.C., Murr L.E., and Nunes A.C. Flow patterns during friction stir welding. *Materials Characterization*, 49:95–101, 2003.

Hoffman E.K., Hafley R.A., Wagner J.A., and Jegley D.C. Compression buckling behavior of large-scale friction stir welded and riveted 2090-T83 Al-Li alloy skin-stiffener panels, TM-2002-211770. Technical Report, NASA, Langley Research Center, Hampton, Virginia, 2002.

Lemmen H.J.K., Alderliesten R.C., and Benedictus R. Fatigue initiation behaviour throughout friction stir welded joints in AA2024-T3. *International Journal of Fatigue*, 32:1928–1936, 2010.

Liu H.J., Fujii H., Maeda M., and Nogi K. Tensile properties and fracture locations of friction-stir-welded joints of 2017-T351 aluminum alloy. *Journal of Materials Processing Technology*, 142:692–696, 2003.

MSC. *Quick Reference Guide*. MSC Software Corporation, 2008.

Murphy A., Lynch F., Price M., and Gibson A. Modified stiffened panel analysis methods for laser beam and friction stir welded aircraft panels. *Journal of Aerospace Engineering*, 220:267–278, 2006.

Murphy A., McCune W., Quinn D., and Price M. The characterisation of friction stir welding process effects on stiffened panel buckling performance. *Thin-Walled Structures*, 45:339–351, 2007.

Swift T. *Fracture Mechanics Design Methodology, AGARD Lecture Series No. 97*. Advisory Group for Aerospace Research and Development, 1979.

Yoon J.W., Bray G.H., Valente R.A.F., and Childs T.E.R. Buckling analysis for an integrally stiffened panel structure with afriction stir weld. *Thin-Walled Structures*, 47:1608–1622, 2009.